Eosinophils orchestrate cancer rejection by normalizing tumor vessels and enhancing infiltration of CD8+ T cells

Rafael Carretero¹, Ibrahim M Sektioglu¹, Natalio Garbi^{1,4}, Oscar C Salgado¹, Philipp Beckhove^{2,3} & Günter J Hämmerling¹

Tumor-associated eosinophilia is frequently observed in cancer. However, despite numerous studies of patients with cancer and mouse models of cancer, it has remained uncertain if eosinophils contribute to tumor immunity or are mere bystander cells. Here we report that activated eosinophils were essential for tumor rejection in the presence of tumor-specific CD8+ T cells. Tumor-homing eosinophils secreted chemoattractants that guided T cells into the tumor, which resulted in tumor eradication and survival. Activated eosinophils initiated substantial changes in the tumor microenvironment, including macrophage polarization and normalization of the tumor vasculature, which are known to promote tumor rejection. Thus, our study presents a new concept for eosinophils in cancer that may lead to novel therapeutic strategies.

Eosinophils are known to express a large number of different cell-surface receptors, including adhesion molecules, Fc receptors, Toll-like receptors, pattern-recognition receptors, and receptors for cytokines and chemokines. They also produce a wide range of immunologically active factors such as type 1 and type 2 cytokines and chemokines ^{1–4}. Moreover, eosinophils exhibit cytotoxic activity that is mediated by secretory granules. Thus, they are equipped to perform different functions, probably depending on the nature of the respective activation signals. It is believed that eosinophils are important for tissue repair and homeostasis, but they participate also in immune responses, such as the clearance of parasites (such as helminths), and the regulation of a variety of diseases, including allergic asthma and autoimmune disorders.

Tumor-associated eosinophilia, first described in 1893 (ref. 5), is frequently observed in patients with cancer. Several studies have shown that eosinophils are attracted into tumors by chemotactic factors^{6,7} such as eotaxins and damage-associated molecular patterns, notably the alarmin HMGB1, which is released by necrotic tumor cells⁸. However, the role of tumor-associated tissue eosinophilia is not clear. Animal studies addressing potential functions of eosinophils in tumors have provided conflicting results^{9–11}. For example, published studies showed that tumor cells engineered to secrete interleukin 4 (IL-4) elicited an eosinophilic granulocyte infiltrate^{12,13}. It was assumed that the infiltrating eosinophils would impede tumor growth via their cytocidal potential¹². That view was challenged by studies of *Il5*^{-/-} mice lacking eosinophils, in which the growth of tumor cells transfected to express IL-4 was impaired as much as it was in wild-type mice¹⁴. Thus, eosinophils were not responsible for

the impairment of tumor growth, which was attributed instead to tumor-infiltrating granulocytic neutrophils 14 . In another study, it was shown that IL-4-driven T helper type 2 ($T_{\rm H}2$) responses mobilized eosinophils that prevented metastasis formation in the B16 mouse melanoma model, but in contrast to the abovementioned report of IL-4-expressing tumor cells 12 , the primary tumor was not affected 15 . Moreover, in studies of tumor cells transfected to express eotaxin or IL-5, despite substantial infiltration of eosinophils, no retardation of tumor growth was observed 16,17 . Thus, these and other mouse studies failed to demonstrate a clear role for eosinophils in tumors.

Clinically, tumor-associated tissue eosinophilia has been reported in many studies to be related to a good prognosis in, for example, gastrointestinal cancers, head and neck cancer, bladder cancer and prostate cancer^{9–11}. In contrast, in the case of Hodgkin lymphoma, oral squamous cell carcinoma and cervical carcinoma, eosinophils have been linked to a poor prognosis^{9–11}. However, most of those studies concentrated solely on the correlation of tumor-associated tissue eosinophilia with clinical outcome and did not evaluate the infiltration of other cells of the immune system, such as T cells. In addition, infiltration and degranulation of eosinophils has been frequently observed during clinical immunotherapy with cytokines such as IL-2, IL-4 and GM-CSF^{9,18,19}, but again a direct tumoricidal effect of eosinophils has been only suggested but not formally shown.

Thus, the function of eosinophils in cancer has remained elusive. However, the studies mentioned above were performed in the absence of a T cell response to the tumor and were focused mainly on a potential direct effect of eosinophils on tumor growth. Subsequently, it has become apparent that cells of the innate immune system are involved

¹Division of Molecular Immunology, German Cancer Research Center, Heidelberg, Germany. ²Division of Translational Immunology, German Cancer Research Center, Heidelberg, Germany. ³Regensburg Center for Interventional Immunology, University Clinic and University of Regensburg, Regensburg, Germany. ⁴Present address: Institutes of Molecular Medicine and Experimental Immunology, University of Bonn, Bonn, Germany. Correspondence should be addressed to G.J.H. (hammerling@dkfz.de).

Received 17 February; accepted 26 March; published online 27 April 2015; corrected after print 21 May 2015 and 13 November 2015; doi:10.1038/ni.3159



in the regulation of adaptive immunity. This regulation has also been observed in the tumor microenvironment, where macrophages have been found to locally control T cell–mediated tumor immunity 20 . Therefore, we explored here whether eosinophils might serve as accessory cells that would contribute to tumor-specific T cell responses. Our study found that eosinophils supported tumor rejection, but only when stringent requirements were fulfilled, such as activation of eosinophils and the presence of tumor-specific CD8+T cells. Under these conditions, activated eosinophils modulated the tumor microenvironment and substantially improved the infiltration of T cells into the tumor, which enhanced tumor rejection and survival. In contrast, in the absence of a T cell response, eosinophils failed to exhibit substantial anti-tumor activity.

RESULTS

Depletion of regulatory T cells induces tumor eosinophilia

To investigate a potential role for eosinophils in tumor rejection, we used in a first set of experiments a tumor model in which CD8+ T cellmediated rejection was accompanied by the infiltration of eosinophils. Efficient CD8+ T cell–dependent rejection of tumors occurred upon depletion of Foxp3+CD4+ regulatory T cells (T_{reg} cells) in Foxp3. LuciDTR-4 mice (which coexpress enhanced green fluorescent protein and luciferase, as well as the diphtheria toxin receptor (DTR),

and thus undergo ablation of T_{reg} cells when treated with diphtheria toxin) bearing large tumors such as MO4 (a B16 melanoma line that expresses full-length ovalbumin)²¹ (**Fig. 1a**). To compare tumors of similar size, we always performed analyses at the onset of tumor rejection in experimental groups and on the same day in control groups, usually day 13. Flow cytometry showed that after depletion of T_{reg} cells, leukocyte infiltration was enhanced two- to threefold (**Fig. 1b,c**), with particular enrichment for CD8⁺ T cells displaying an activated phenotype (**Fig. 1d**). Notably, tumor rejection was associated with prominent infiltration of eosinophils (**Fig. 1c**), which represented about 8% of the total infiltrate of cells of the immune system.

Eosinophils were characterized as CD11b+Gr-1loF4/80+ cells (Supplementary Fig. 1). These markers are also found on macrophages, but eosinophils can be distinguished from macrophages due to their high granularity, lack of expression of major histocompatibility complex class II (MHCII) and expression of the sialic acid-binding lectin Siglec-F (Fig. 1e). Siglec-F is prominent on mouse eosinophils and is the paralog to the human eosinophil-specific marker Siglec-8 (ref. 22). For more thorough characterization, we sorted tumor-derived eosinophils for further analysis of eosinophil-specific transcripts by real-time PCR. Sorted intra-tumor CD11b+Gr-1loF4/80+Siglec-F+ cells had abundant expression of *Mbp* and *Epo* mRNA, which encode the eosinophil-specific major basic protein and eosinophil peroxidase,

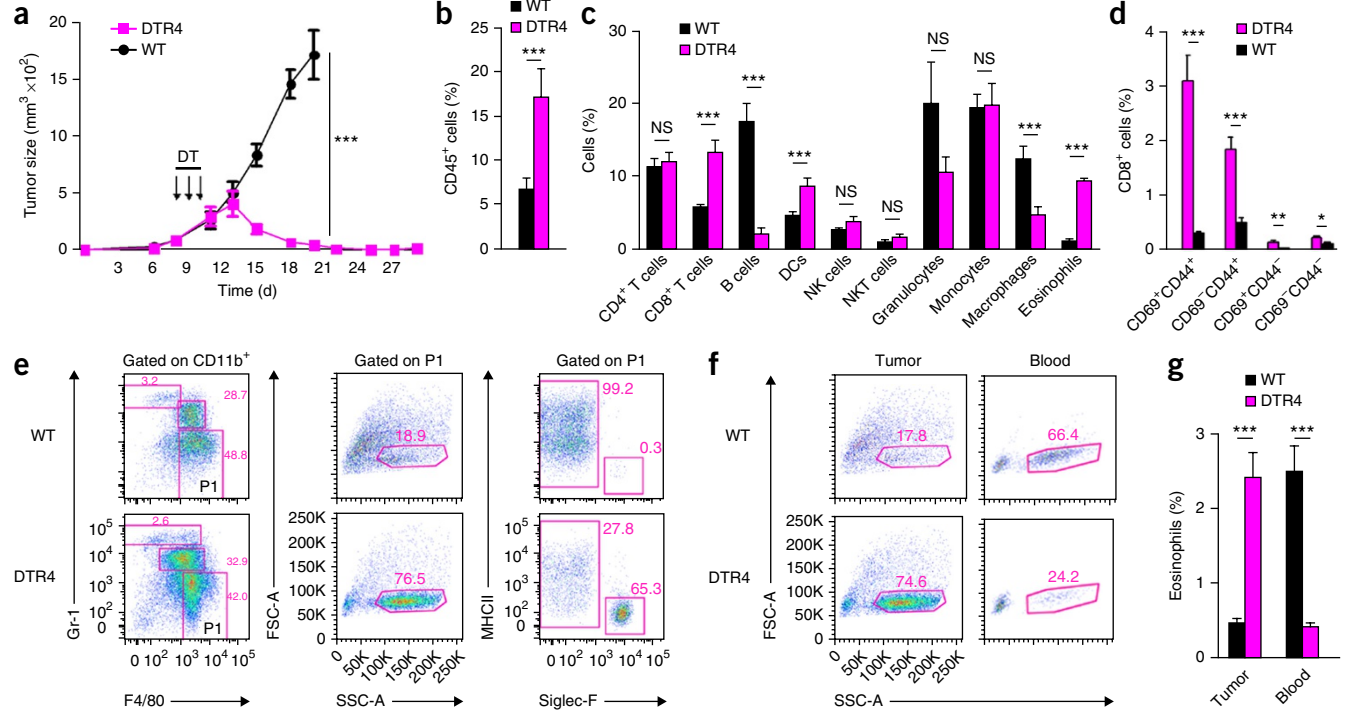


Figure 1 T_{reg} cell depletion results in eosinophil infiltration and tumor rejection. (a) Growth of MO4 tumors in wild-type mice (WT) and Foxp3.Luci-DTR-4 C57BL/6N mice (DTR4) given subcutaneous injection of MO4 tumor cells and then treated with diphtheria toxin (DT) on days 8–11 (downward arrows), followed by tumor isolation for analysis on day 13. (b) Quantification of total infiltration of CD45+ leukocytes into MO4 tumors in mice as in a at the onset of tumor rejection 13 d after tumor inoculation (5 d after the first injection of diphtheria toxin), analyzed by flow cytometry. (c) Quantification of the infiltration of specific leukocyte subpopulations (horizontal axis) into MO4 tumors on day 13 after tumor inoculation as in a (gating strategy, Supplementary Fig. 1). DC, dendritic cell; NK, natural killer. (d) Activation status of tumor-infiltrating CD8+ T cells on day 13 in mice as in a. (e) Flow cytometry of tumor-infiltrating cells from mice as in a, characterized as CD11b+Gr-1loF4/80+Siglec-F+MHCII-FSCloSSChi eosinophils. Numbers adjacent to outlined areas indicate percent Gr-1hiF4/80- cells (top left), Gr-1hiF4/80+ cells (top right) or Gr-1loF4/80+ (P1) cells (bottom right) (left column); percent Gr-1loF4/80+ (P1) cells with low forward scatter and high side scatter (FSCloSSChi) (middle column); and percent MHCII-Siglec-F+P1 cells (right) (right column). (f) Flow cytometry of cells from tumors and peripheral blood of mice as in a. Numbers adjacent to outlined areas indicate FSCloSSChi eosinophils. (g) Frequency of eosinophils in tumor and blood, calculated from results in e,f. NS, not significant (P>0.05); *P<0.05, **P<0.01 and ***P<0.001 (two-tailed analysis of variance (ANOVA) (a) or unpaired t-test (b-d,g)). Data are from one experiment representative of three independent experiments (mean and s.e.m. of n = 6 mice per group in a-d,g).



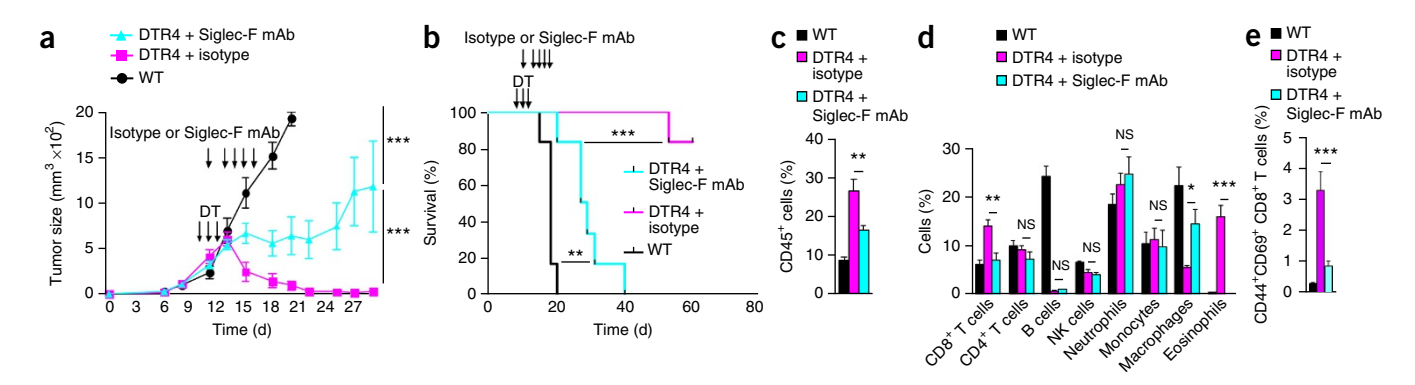


Figure 2 Tumor rejection after T_{reg} cell depletion is dependent on infiltrating eosinophils. (a) Growth of MO4 tumors in wild-type C57BL/6N mice given injection of MO4 tumor cells and then treated with diphtheria toxin (DT with downward arrows) alone (WT) or in Foxp3.Luci-DTR-4 mice given injection of MO4 tumor cells and then treated with diphtheria toxin (for depletion of T_{reg} cells) plus isotype-matched control (irrelevant) antibody (DTR4 + isotype) or monoclonal antibody to Siglec-F (for ablation of eosinophils) (DTR4 + Siglec-F mAb) (top downward arrows). (b) Survival of mice treated as in a. (c) Frequency of total tumor-infiltrating CD45+ leukocytes in mice as in a. (d) Frequency of tumor-infiltrating leukocyte subpopulations in mice as in a. (e) Frequency of tumor-infiltrating activated (CD44+CD69+) CD8+T cells among CD45+ cells in mice as in a. *P < 0.05, *P < 0.01 and ***P < 0.001 (two-tailed ANOVA (a), log-rank (Mantel-Cox) test (b) or unpaired t-test (c-e)). Data are from one experiment representative of three independent experiments (mean and s.e.m. of P = 0.001 mice per group).

respectively (**Supplementary Fig. 2a**). In addition, tumor-associated eosinophils stained with hematoxylin and eosin exhibited the characteristic eosinophil morphology, with a lobulated nucleus and eosinophilic granules (**Supplementary Fig. 2b**). After depletion of T_{reg} cells, eosinophils migrated into the tumor, which led to a reduction in their number in blood and an increase in their number in the tumor (**Fig. 1f,g**). Therefore, tumor rejection after the depletion of T_{reg} cells was associated with substantial infiltration of eosinophils.

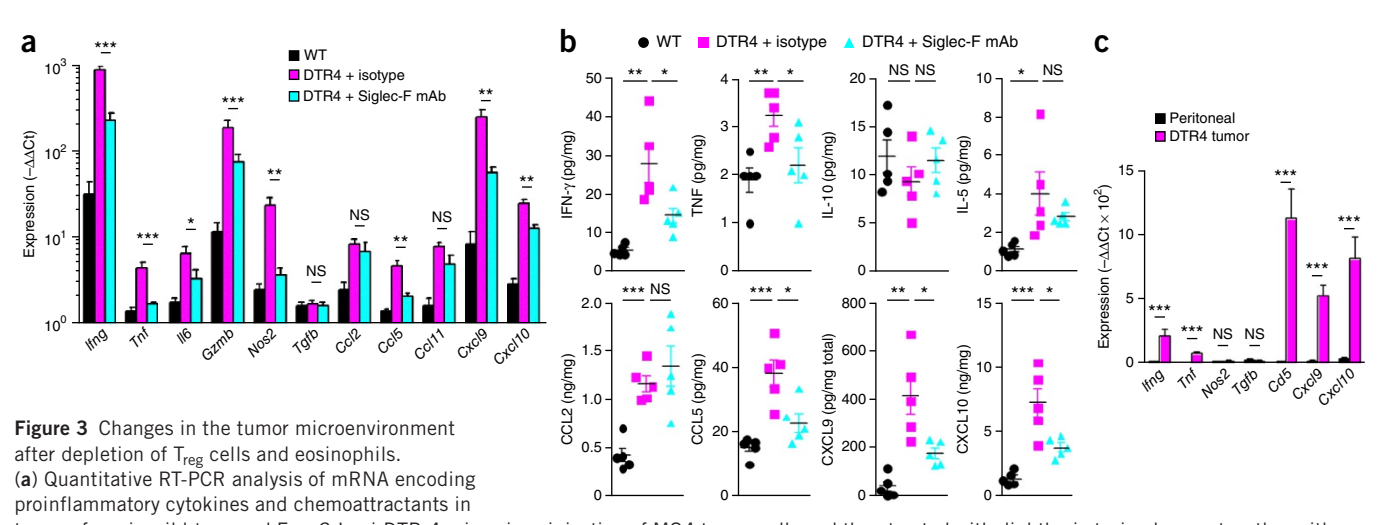
Eosinophils are essential for efficient tumor rejection

To study the role of eosinophils in tumor rejection, we used a Siglec-F-specific monoclonal antibody that has been shown to specifically cause depletion of eosinophils via the induction of apoptosis^{22,23}. Mice underwent efficient depletion of eosinophils in lymph nodes and tumor after a single injection of the monoclonal antibody to Siglec-F

(Supplementary Fig. 3). Tumor rejection was significantly impeded in the absence of eosinophils (Fig. 2a), which resulted in severely reduced survival (Fig. 2b). To elucidate the underlying mechanism of this, we investigated the composition of cells of the immune system in the tumors before and after eosinophil depletion. The depletion of eosinophils resulted in impaired infiltration of CD45⁺ leukocytes into the tumor (Fig. 2c). The reduction in the number of activated CD8⁺ T cells was especially substantial (Fig. 2d,e). This finding probably explained the abrogation of tumor rejection in the absence of eosinophils. These results indicated a role for eosinophils in CD8⁺ T cell–mediated tumor rejection.

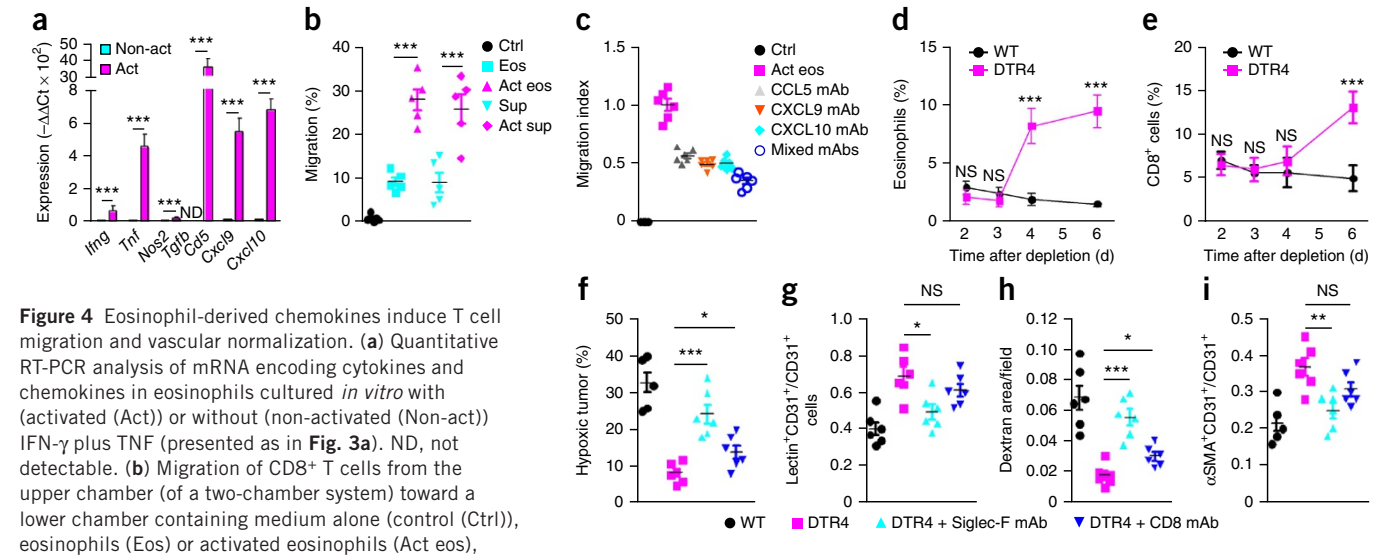
Eosinophils induce inflammation and T cell migration

Next we analyzed the cytokine and chemokine profiles of the tumor microenvironment in the presence and absence of eosinophils.



tumors from in wild-type and Foxp3.Luci-DTR-4 mice given injection of MO4 tumor cells and then treated with diphtheria toxin alone or together with isotype-matched control antibody or monoclonal antibody to Siglec-F (as in **Fig. 2a**); results were calculated by the change-in-cycling-threshold ($\Delta\Delta$ Ct) method, relative to those of *Gapdh* mRNA (control gene). (**b**) Multiplex analysis of cytokines and chemokines in the tumors from mice as in **a**. Each symbol represents an individual mouse; small horizontal lines indicate the mean (\pm s.e.m.). (**c**) Quantitative RT-PCR analysis of mRNA encoding proinflammatory cytokines and chemoattractants in peritoneal eosinophils isolated 3 days after intraperitoneal injection of thioglycollate (Peritoneal) and in tumor-infiltrating eosinophils isolated on day 13 from tumor-bearing Foxp3.Luci-DTR-4 mice treated with diphtheria toxin (DTR4 tumor); results presented as in **a**. *P < 0.05, **P < 0.01 and ***P < 0.001 (unpaired t-test). Data are from one experiment representative of three (**a**,**c**) or two (**b**) independent experiments (mean and s.e.m. of n = 6 (**a**,**c**) or 5 (**b**) mice per group).





or supernatants of eosinophils (Sup) or of activated eosinophils (Act sup). (c) Migration of CD8+ T cells in a system as in b, toward a lower chamber containing medium alone, activated eosinophils or monoclonal antibody (mAb) to CCL5, CXCL9 or CXCL10 or a mixture of monoclonal antibodies to all three (Mixed mAbs). (d,e) Kinetics of the infiltration of eosinophils (d) and CD8+ T cells (e) into tumors from MO4 tumor-bearing wild-type and Foxp3-LuciDTR4 mice treated with diphtheria toxin 8 d after tumor inoculation (as in Fig. 1a). (f) Tumor hypoxia in mice treated as in d,e, followed by no additional treatment or treatment with mAb to Siglec-F or CD8 (key), assessed by pimonidazole staining. (g) Vessel perfusion of tumors from mice as in f, assessed by localization of the adhesion molecule CD31 (PECAM-1) together with injected FITC-labeled tomato lectin, presented as the ratio of lectin-positive CD31+ cells to CD31+ cells (Lectin+CD31+/CD31+). (h) Vascular leakiness of tumors from mice as in f, assessed by injection of FITC-labeled dextran. (i) Pericyte-endothelial cell association, assessed by the localization of CD31 together with the mature pericyte marker α -smooth muscle actin, presented as the ratio of α -smooth muscle actin-positive CD31+ cells to CD31+ cells (α SMA+CD31+/CD31+). Each symbol (b,c,f-i) represents an individual mouse; small horizontal lines indicate the mean (± s.e.m.). *P < 0.05, **P < 0.01 and ***P < 0.001 (unpaired t-test). Data are from one experiment representative of three (a-e; mean and s.e.m. of n = 5 (a,b) or 6 (c-e) mice per group) or are from one experiment (f-i; mean and s.e.m. of n = 6 mice per group (f-i); whole tumor area (f) or average of ten randomly selected intra-tumor fields from each tumor (g-i)).

Depletion of T_{reg} cells induced considerable activation of genes encoding proinflammatory factors such as interferon- γ (IFN- γ), tumor-necrosis factor (TNF) and IL-6, chemokines such as CCL5, CCL11, CXCL9 and CXCL10, and the effector molecules inducible nitric oxide synthase and granzyme B (**Fig. 3a**). After depletion of eosinophils, the upregulation of these genes was significantly impaired, particularly the upregulation of those encoding CCL5, CXCL9 and CXCL10, which are known to be potent chemoattractants for CD8+ T cells (**Fig. 3a**). We observed the greatest reduction in the expression of genes encoding TNF, CCL5 and inducible nitric oxide synthase (**Fig. 3a**). We confirmed those results at the protein level by multiplex analysis (**Fig. 3b**). Eosinophils sorted from tumors depleted of T_{reg} cells produced large amounts of the abovementioned chemokines (**Fig. 3c**), which suggested that eosinophils were an important source of these intra-tumor factors.

The observed production of chemokines such as CCL5, CXCL9 and CXCL10 by tumoral eosinophils raised the possibility that CD8+ T cells might be attracted into the tumor by these chemoattractants, which would explaining the reduced infiltration of T cells in the absence of eosinophils. We investigated the effect of eosinophils on T cell migration in a two-chamber system *in vitro*. Purified eosinophils activated *in vitro* with IFN-γ and TNF (**Supplementary Fig. 4**) produced large amounts of CCL5, CXCL9 and CXCL10, but eosinophils that were not activated did not (Fig. 4a and Supplementary Fig. 5a). Activated eosinophils were able to induce the migration of activated CD8+ T cells, with activated eosinophils or supernatants thereof being superior to non-activated cells in this induction (Fig. 4b and Supplementary Fig. 5b). Blockade of CCL5, CXCL9 and CXCL10 with specific antibodies inhibited the migration of CD8+T cells (Fig. 4c), which indicated that these chemokines, and possibly others, were indeed responsible for attracting T cells. Kinetic studies of the infiltration of tumors by leukocyte subpopulations revealed that infiltration by eosinophils preceded infiltration by CD8+

T cells (**Fig. 4d,e**), in agreement with the notion that eosinophils critically contributed to the homing of T cells to the tumor.

Depletion of T_{reg} cells induces normalization of the tumor vasculature, which is known to promote T cell infiltration^{21,24}. The additional depletion of eosinophils by the Siglec-F-specific antibody resulted in increased tumor hypoxia, which demonstrated that eosinophils were important for the normalization process. We assessed hypoxia by intraperitoneal injection of pimonidazole, which localizes in hypoxic tumor areas and can be visualized by staining with specific antibodies (Fig. 4f and Supplementary Fig. 6). Depletion of eosinophils also increased vascular leakiness and diminished vascular perfusion, as well as the coverage of vessels with mature pericytes (Fig. 4g-i and Supplementary Fig. 6). We measured vascular perfusion by intravenous injection of tomato lectin, which stains all vessels with an active perfusion (Fig. 4g and Supplementary Fig. 6). We assessed vascular leakiness by intravenous injection of fluorescein isothiocyanate (FITC)-labeled dextran, which leaks out of the vasculature when there is a vessel rupture (Fig. 4h and Supplementary Fig. 6). Coverage of vessels with mature pericytes was shown by staining with antibody to α-smooth muscle actin (Fig. 4i and Supplementary Fig. 6). In contrast, ablation of CD8+ T cells had only a minor effect on vascular normalization (Fig. 4f-i and Supplementary Fig. 6). The finding of normalization in the presence of eosinophils was unexpected, because these cells are known to produce pro-angiogenic cytokines that can induce vessel formation in vitro²⁵. This apparent discrepancy can be explained by our finding that activation of eosinophils in vitro by IFN-γ decreased the production of most angiogenic factors, such as VEGF, FGF, PLGF and Ang-2 (Supplementary Fig. 5c). These data indicated that activated eosinophils substantially induced normalization of the tumor vasculature and T cell migration through the production of cytokines and chemokines.



Eosinophils promote tumor rejection by attracting CD8+ T cells

In the clinic, adoptive T cell transfer has emerged as a promising approach, but its success is still limited²⁶. Therefore, we investigated whether eosinophils would be able to improve the efficacy of T cell therapy. Moreover, the use of cell transfer allowed us to study in more detail the mechanism by which eosinophils support tumor immunity. The transfer of activated tumor-specific OT-I T-cells (with transgenic expression of an MHC class I-restricted (ovalbumin-specific) T cell antigen receptor) into wild-type C57BL/6 mice bearing large

established tumors resulted in only mild inhibition of tumor growth (Fig. 5a). In contrast, the transfer of T cells together with purified activated eosinophils led to much greater inhibition of tumor growth and significantly extended mouse survival (Fig. 5a,b). Transferred eosinophils accumulated 'preferentially' in the tumor and, to a lesser extent, in liver, spleen and lymph nodes (Fig. 5c). The transfer of T cells together with eosinophils that had not been activated failed to inhibit tumor growth (Fig. 5a), which demonstrated that eosinophils needed to be activated to exert anti-tumor activity. We observed only

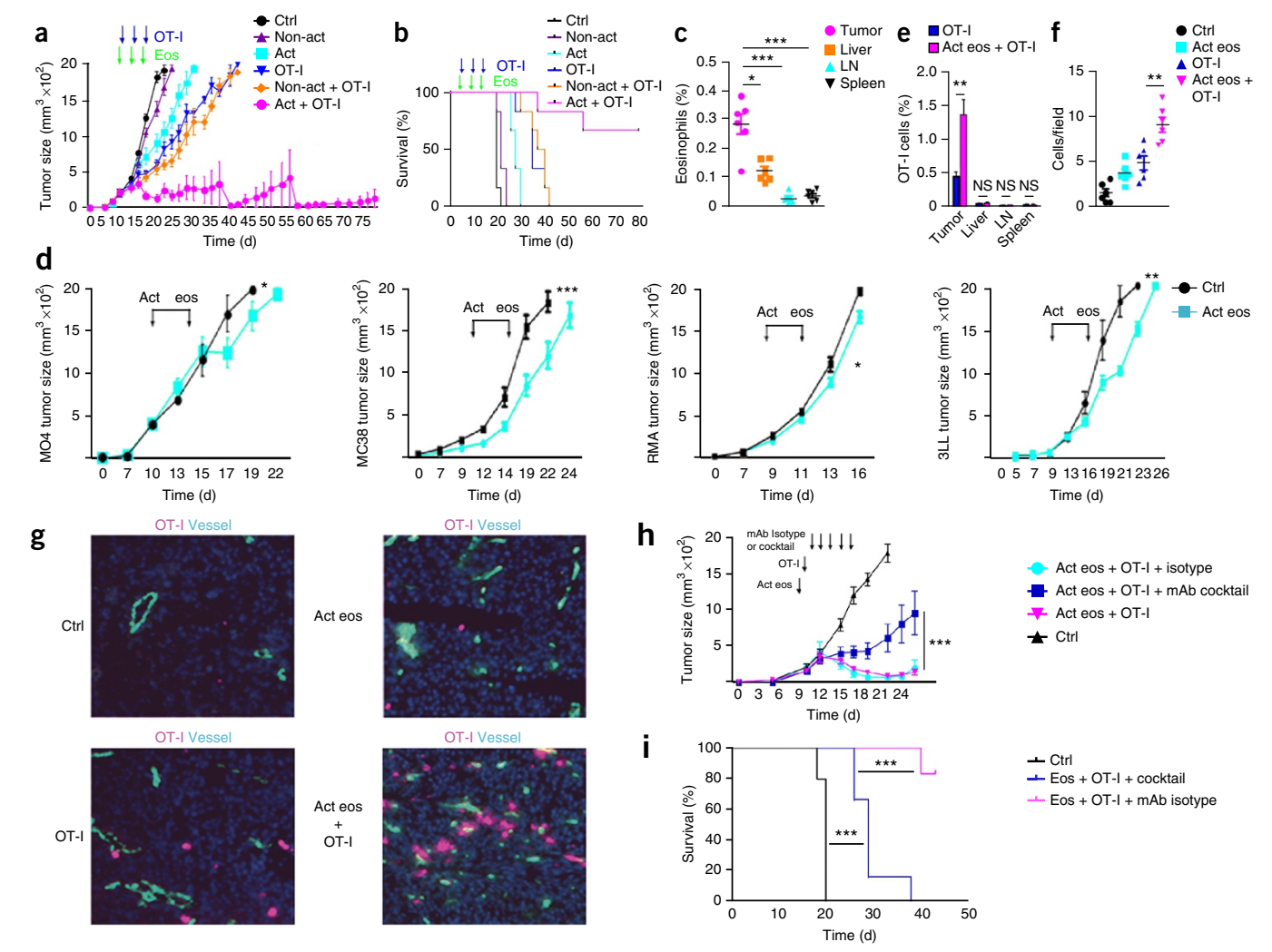
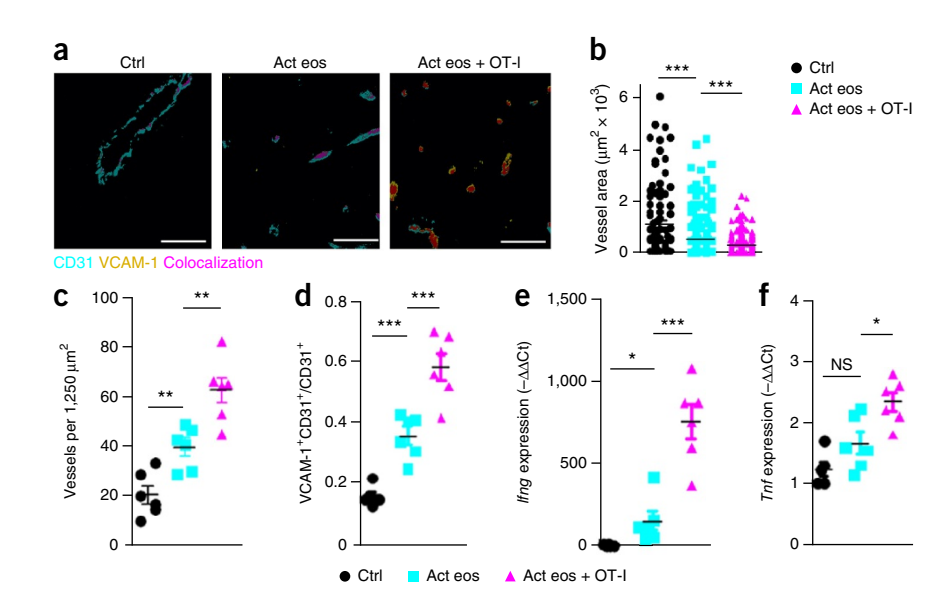


Figure 5 Adoptive transfer of tumor-specific CD8+T cells alone fails to reject tumors, whereas transfer of those cells together with activated eosinophils leads to substantial T cell infiltration and tumor rejection. (a) Tumor growth after adoptive transfer of no cells (control (Ctrl)) or various combinations (key) of non-activated eosinophils (Non-act), activated eosinophils (Act) and/or activated OT-I CD8+T cells at various times (downward arrows) into mice bearing established MO4 tumors. Eos, eosinophils. (b) Survival of mice as in a. (c) Recovery of transferred eosinophils from the tumor, liver, lymph nodes (LN) and spleen of mice as in a given transfer of activated eosinophils together with OT-I CD8+ T cells, analyzed by flow cytometry 2 d after eosinophil transfer and presented as frequency of eosinophils among total tissue cells. (d) Tumor growth in T cell-deficient Rag2-/- mice given inoculation of MO4, MC38, RMA or 3LL tumor cells and no additional cells (Ctrl) or transfer (downward arrows) of activated eosinophils (Act eos). (e) Migration of OT-I CD8+ T cells into MO4 tumors or the liver, lymph nodes and spleen of mice given inoculation of MO4 tumor cells plus OT-I CD8+ T cells alone (OT-I) or together with activated eosinophils (Act eos + OT-I), assessed by cytofluorometry. (f) Infiltration of CD8+T cells into MO4 tumors in mice given inoculation of MO4 tumor cells plus no cells (WT) or activated eosinophils and/or OT-I cells alone or together (key), assessed by evaluation of the immunohistofluorescence in g. (g) Immunohistofluorescence of OT-I CD8+ cells (magenta) and CD31+ tumor vessels (cyan) in tumors from mice as in f. (h) Tumor growth in mice given inoculation of MO4 tumor cells plus no cells (WT) or adoptive transfer (downward arrows) of activated eosinophils or OT-I cells alone or together (key), with no antibody or in combination with isotype-matched control antibody or a 'cocktail' of mAbs to CCL5, CXCL9, CXCL10 (mAb cocktail; top downward arrows). (i) Survival of mice as in h. Each symbol (c,f) represents an individual mouse (n = 6 per group); small horizontal lines indicate the mean (± s.e.m.). *P < 0.05, **P < 0.01 and ***P < 0.001 (unpaired t-test (c,e,f), two-tailed ANOVA (d,h) or log-rank (Mantel-Cox) test (i)). Data are from one experiment representative of three (a-c) or two (e-i) independent experiments (n = 6 mice per group mean and s.e.m. in a,c,e,f,h; mean of ten fields per tumor in f) or are from one experiment (**d**; mean and s.e.m. of n = 6 mice per group).

Figure 6 Cotransfer of cells promotes a reduction in vessel size and increases VCAM-1 expression. (a) Immunohistofluorescence of CD31 and VCAM-1 in tumors (of comparable size) from mice inoculated with MO4 tumor cells plus no additional cells or plus activated eosinophils alone or together with OT-I cells (above images), assessed 2 d after eosinophil transfer and 1 d after T cell transfer, by staining with anti-CD31 (turquoise) and anti-VCAM1 (yellow). Scale bars, 100 µm. (b,c) Quantification of tumor vessel size (b) and tumor vessels (c) in tumors as in a. (d) Expression of VCAM-1 on CD31+ tumor vessels as in a, presented as the ratio of VCAM-1+CD31+ cells to CD31+ cells. (e,f) Quantitative RT-PCR analysis of Ifng (e) and Tnf (f) in lysates of in tumors as in a (presented as in Fig. 3a). Each symbol (b-f) represents an individual mouse (n = 6 per group); small horizontal



lines indicate the mean (\pm s.e.m.). *P < 0.05, **P < 0.01 and ***P < 0.001 (unpaired t-test). Data are from one experiment representative of three (a-d) or two (e,f) (mean and s.e.m. of n = 6 mice per group in b-f; ten fields per tumor in c,f).

minor inhibition of tumor growth when we injected activated eosinophils alone (**Fig. 5a**). Likewise, the transfer of eosinophils into T cell–deficient $Rag2^{-/-}$ mice had only minor effects on the growth of various tumor entities, such as MO4 melanoma, MC38 colorectal carcinoma, RMA thymoma and 3LL lung carcinoma (**Fig. 5d**). Thus, the cytocidal potential of eosinophils did not seem to have a major role in this. Instead, the presence of eosinophils led to increased infiltration of tumor-specific T cells and other leukocytes into the tumor, as shown by flow cytometry (**Fig. 5e** and **Supplementary Fig. 7a**) and immunohistofluorescence (**Fig. 5f,g**). The CD8+ T cells localized together with the co-transferred eosinophils in the tumor (**Supplementary Fig. 7b**). Together these findings were consistent with our results showing that ablation of eosinophils decreased the hom-

ing of T cells into the tumor (**Fig. 2d**). Moreover, *in vivo* blockade of CCL5, CXCL9 and CXCL10 by injection of a 'cocktail' of antibodies to these chemoattractants impaired the tumor rejection obtained by the combination of eosinophils plus T cells (**Fig. 5h,i**), in agreement with our finding that these eosinophil-derived chemokines induced T cell migration (**Fig. 4b,c**). The inhibition was not complete, which left open the possibility that additional chemoattractants were involved.

We confirmed the requirement for activated eosinophils in T cell-mediated tumor rejection in an additional tumor system. For this purpose, we used the melanoma line HCmel1274, isolated from a genetically modified mouse that spontaneously develops melanoma, and pmel CD8⁺ T cells, which have transgenic expression of a T cell antigen receptor specific for the natural melanoma antigen gp100.

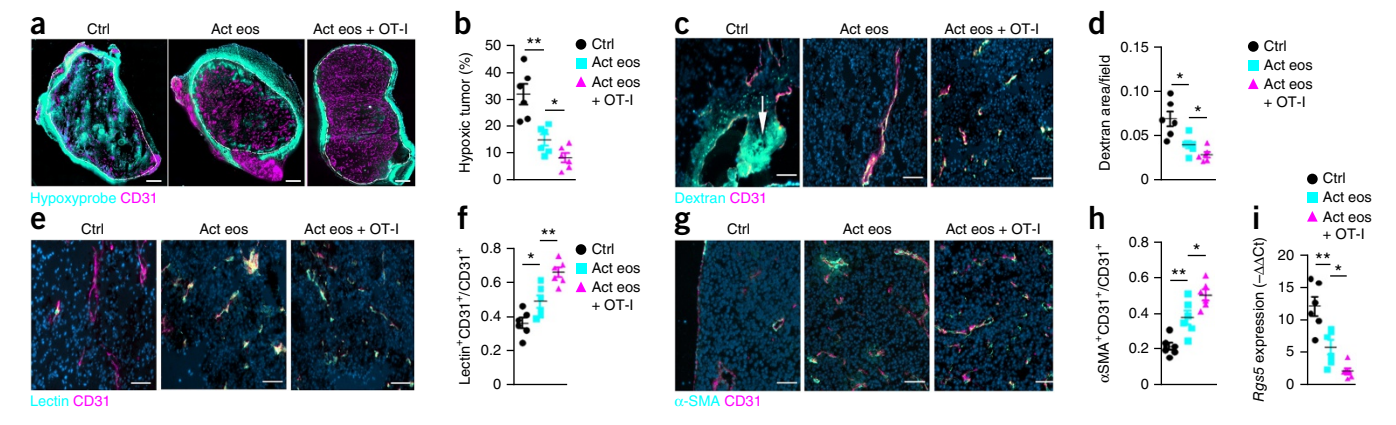
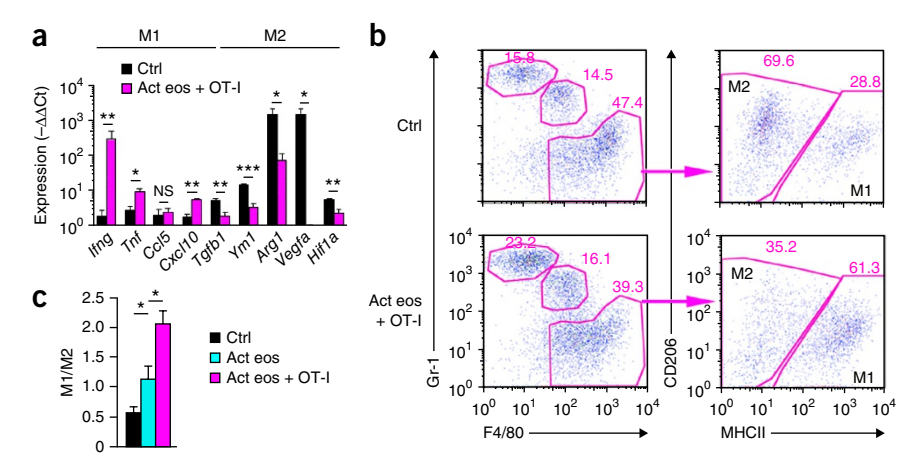


Figure 7 Normalization of tumor vasculature. (a,b) Hypoxia in tumors (of comparable size) from mice inoculated with MO4 tumor cells plus no additional cells or activated eosinophils alone or together with OT-I cells (above images), analyzed 2 d after eosinophil transfer and 1 d after T cell transfer, by stained with the hypoxia marker pimonidazole (Hypoxyprobe) and anti-CD31 (a) and by quantification of hypoxic tumors (b). (c,d) Leakiness of tumors as in a,b, assessed by staining with FITC-labeled dextran (arrow) and anti-CD31 (c) and by quantification of dextran (d). (e,f) Perfusion of tumors as in a,b, assessed by staining with FITC-labeled tomato lectin and anti-CD31 (e) and by quantification of lectin-positive CD31+ cells (as in Fig. 4g) (f). (g,h) Coverage of tumors by mature pericytes in tumors as in a,b, assessed by staining of α -smooth muscle actin and CD31 (g) and by quantification of α SMA+CD31+ cells (as in Fig. 4i) (f). (i) Quantitative RT-PCR analysis of Rgs5 in lysates of tumors as in a,b (presented as in Fig. 3a). Scale bars, 1 mm (a) or 100 μ m (c,e,g). Each symbol (b,d,f,h,i) represents an individual mouse (n = 6) per group); small horizontal lines indicate the mean (\pm s.e.m.). *P < 0.005, **P < 0.01 and ***P < 0.001 (unpaired t-test). Data are from one experiment (a-h; ten fields per tumor (c-h)) or are from one experiment representative of two experiments (i).



Figure 8 Cotransfer of cells results in the M1-like polarization of tumor-associated macrophages. (a) Quantitative RT-PCR analysis of mRNA encoding cytokines and chemokines that serve as markers for M1- and M2-like macrophages in macrophages sorted from tumors of mice inoculated with MO4 tumor cells plus no additional cells (WT) or activated eosinophils together with OT-I cells (presented as in Fig. 3a). (b) Flow cytometry of tumor macrophages (identified as CD11b+CD11c-F4/ 80+Gr-1- cells; left), sorted as M1- and M2-like macrophages (right). Numbers adjacent to outlined areas indicate percent Gr-1hiF4/80cells (top left), Gr-1hiF4/80+ cells (middle) or Gr-1-F4/80+ cells (bottom right) (left) or percent CD206-MHCIIhi M1-like macrophages (M1) or CD206+MHCII^{lo} M2-like macrophages



(M2) (right). (c) Ratio of M1-like macrophages to M2-like macrophages (M1/M2) in tumors from mice inoculated with tumor cells plus no additional cells (WT) or activated eosinophils alone or together with OT-I cells (key). *P < 0.05, **P < 0.01 and ***P < 0.001 (unpaired t-test). Data are from one experiment representative of two experiments (mean and s.e.m. n = 6 mice per group in a,c).

Again, we observed efficient tumor rejection and prolonged survival of mice after intravenous co-transfer of T cells with activated eosinophils (Supplementary Fig. 8). Together these data demonstrated that eosinophils promoted tumor rejection via the attraction of T cells and not by direct killing of tumors.

Vasculature normalization and macrophage polarization

The effect of eosinophils was not limited to the recruitment of leukocytes. We observed that the intravenous transfer of eosinophils and T cells together into MO4 tumor-bearing mice caused considerable changes in the tumor microenvironment, including vessel normalization and reprogramming of tumor associated macrophages (Fig. 6). Untreated tumors showed aberrant vasculature characterized by few but dilated vessels (Fig. 6a). Eosinophils alone significantly induced normalization of the vasculature, an effect that was further enhanced by the co-transfer of T cells and resulted in replacement of large dilated vessels by a large number of small vessels (Fig. 6a-c). The normalized vessels displayed increased expression of adhesion molecules such as VCAM-1 (CD106) (Fig. 6a,d), which could be explained by the observed increased in intra-tumor expression of *Ifng* and *Tnf* (**Fig. 6e,f**).

Normalization of the tumor vasculature after intravenous transfer of eosinophils and T cells together was further evident from various parameters typically measured in these analyses²⁷, including diminished hypoxia (Fig. 7a,b), reduced vascular leakiness and increased vascular perfusion (Fig. 7c-f), increased coverage of vessels with mature pericytes (Fig. 7g,h), and lower expression of Rgs5 (which encodes a regulator of G protein signaling), another indicator of vessel normalization (Fig. 7i). RGS5 is involved in causing the formation of abnormal tumor vasculature and therefore has high expression on abnormal tumor vessels but not on normalized tumor vessels²⁴. Usually normalization is not associated with an increase in vessel number, as observed here (Fig. 6c). Possibly the ongoing immune response to the tumor supported enhanced vessel formation by as-yet-unknown mechanisms. In addition to vascular normalization, the intra-tumor cytokine profile was modified toward a more pro-inflammatory milieu (Supplementary Fig. 7c). However, in contrast to the expression of pro-inflammatory cytokines, the expression of angiogenic factors (such as VEGF, FGF, PGF, Ang-2, etc.) was decreased after the transfer of eosinophils together with T cells (Supplementary Fig. 7d), consistent with the observed vascular normalization.

Notably, macrophages sorted from MO4 tumors after the co-transfer of eosinophils and CD8+ T cells displayed an M1 like phenotype, with higher expression of *Ifng*, *Tnf* and *Cxcl10* and lower expression of genes encoding M2 markers, such as Tgfb, Ym1 and Arg1, than that of macrophages from untreated tumor-bearing mice (Fig. 8a). For a more quantitative evaluation, we used flow cytometry to determine the ratio of CD206hiMHCIIlo M2-like macrophages to CD206loMHCIIhi M1-like macrophages (**Fig. 8b**). In untreated tumors, the majority of macrophages were M2 like, whereas tumors from mice that received eosinophils plus T cells contained mainly M1-like macrophages (**Fig. 8c**). The macrophage polarization probably depended on IFN- γ^{28} induced by the transfer of eosinophils and T cells (Fig. 6e) and might explain the observed vessel normalization, because M2-like macrophages are important producers of tumor-angiogenesis factors such as VEGF and HIF- $1\alpha^{29,30}$, whereas the expression of genes encoding such factors was considerably lower in M1-like macrophages than in M2-like macrophages (Fig. 8a). In conclusion, the transfer of eosinophils together with T cells induced normalization of the vasculature and M1 skewing of tumor-associated macrophages.

DISCUSSION

In clinical and animal studies of eosinophils in cancer, these cells have usually been perceived as innate host-defense cells with nonspecific destructive activities that eliminate cancer cells. Since eosinophils have been found to be able to destroy tumor cells in vitro via their cytocidal granules, this concept was plausible, but data demonstrating directly in vivo destruction of tumors by eosinophils have been missing.

In the present study we have addressed this long-standing question and propose a new concept for eosinophils in cancer. By using adoptive transfer of eosinophils into tumor-bearing animals, we observed that activated eosinophils migrated mainly into tumors and to a much lesser extent into other tissues such as lymphoid organs or liver. This 'preferential' tumor homing was probably due to the release of damage-associated molecular patterns by necrotic tumor areas, which are known to be powerful chemoattractants for eosinophils^{8,9}. Thus, we were able to mimic tumor-associated tissue eosinophilia. However, despite considerable infiltration of eosinophils, we observed only minor effects on tumor growth for several distinct tumors types growing in wild-type and T cell-deficient Rag2-/- mice. At present it is not clear if these small effects were due to direct cytotoxicity of eosinophils or were due to other mechanisms that would affect tumor

growth, such as the activation of natural killer cells. Nevertheless, together the results indicated that eosinophils did not act as a major destructive cell type in tumors.

Instead, we found that eosinophils served as critical accessory cells for the attraction of tumor-specific CD8+ T cells. Activated tumor-infiltrating eosinophils produced large amounts of chemokines, such as CCL5, CXCL9 and CXCL10, that recruited co-transferred CD8+ T cells to the tumor, which resulted in tumor rejection and prolonged survival. The importance of these chemokines was underscored by the finding that we observed recruitment of T cells only when they were transferred together with activated eosinophils, but not after transfer together with non-activated eosinophils that failed to produce chemoattractants. Moreover, blockade of the abovementioned chemokines by specific antibodies impeded T cell migration and tumor rejection, but at present the possibility of the involvement of additional chemoattractants cannot be ruled out.

Beyond the attraction of T cells toward the tumor, additional mechanisms are required that provide access into the tumor. Our results demonstrated the effect of eosinophils was not limited to T cell recruitment. Co-transfer of eosinophils and T cells led also to considerable changes in the tumor microenvironment, including normalization of the tumor vasculature and macrophage polarization. Both processes are known to support the infiltration and activity of T cells. Unlike the vessels of normal tissue, tumors vessels are highly irregular. Driven by the incessant production of proangiogenic factors such as VEGF, solid tumors develop a structurally and functionally abnormal vasculature characterized by dilated and tortuous vessels, which results in tumor hypoxia and high interstitial fluid pressure³¹. These abnormalities have been shown to impair the infiltration of effector T cells into tumors³¹⁻³³ but not the infiltration of immunosuppressive cells such as T_{reg} cells, macrophages and myeloid cells^{34,35}. In contrast, a normalized tumor vasculature has been found to facilitate T cell infiltration and tumor rejection. Normalization can be achieved by various approaches, including the deletion of Rgs5 (ref. 24), the induction of a pro-inflammatory microenvironment (for example, by local irradiation 32,36 or treatment with Toll-like receptor ligands³⁷), or the efficient depletion of T_{reg} cells²¹. A normalized vasculature has smaller vessels characterized by decreased leakiness, improved perfusion and diminished hypoxia, which increases the motility and activity of T cells^{24,31,38,39}.

The precise mechanism of tumor vessel normalization and the sequence of events are not clear. Whereas high expression of VEGF is associated with the formation of aberrant vasculature, a reduction in VEGF expression leads to vessel normalization 29,39,40 . Since tumor-associated macrophages seem to be the most important source of VEGF²⁹, we investigated VEGF production by tumor-associated macrophages after transfer of eosinophils alone and observed that eosinophils initiated the polarization of tumor macrophages toward M1-like macrophages, which produce only small amounts of VEGF. Thus, the eosinophil-induced vessel normalization seemed to operate via M1 skewing, which was probably promoted by eosinophil-derived IFN- γ and TNF. On the basis of these observations, we propose the following model in which the partial vasculature normalization and VCAM-1 expression induced by eosinophils enables CD8⁺ T cells to infiltrate: in a feedback mechanism, these early infiltrating T cells lead to more M1 skewing, normalization and VCAM-1 expression and thereby to more T cell infiltration and tumor eradication. Although consistent with the data, this feedback model remains speculative.

Our results help to explain some of the discrepancies in the literature on tumor-associated eosinophilia in patients with cancer and establish the conditions under which eosinophils are able to support

tumor immunity. First, tumor-specific effector T cells need to be present so that they can be attracted by eosinophils into the tumor. Second, for the production of chemoattractants, eosinophils need to be activated. Similar to the M1-M2 concept, eosinophils can be polarized to produce either type 1 or type 2 cytokines, depending on the activation stimulus⁴¹. Thus, eosinophils cultured with IL-4 and TNF activate selectively the STAT6 signaling pathway and produce CCL17 and CCL22, which attract T_H2 cells via binding to the homing receptor CCR4. Conversely, activation of the STAT1 signaling pathway by IFN- γ plus TNF leads to the production of interferon-inducible chemokines such as CXCL9, CXCL10 and CXCL11, which attract TH1 cells. Probably only eosinophils activated by factors that are part of a T_H1 response would recruit CD8+ effector T cells into tumors, but T_H2 factor-activated or non-activated eosinophils would not. As T_H2 factor-activated eosinophils are critical for sustaining alternatively activated M2-like macrophages in adipose tissue⁴², they probably also maintain M2-like macrophages in tumors and thereby promote an immunosuppressive and pro-tumorous environment.

In conclusion, the mere presence of eosinophils cannot be used as a prognostic factor in clinical studies without determination of the precise activation and polarization status of eosinophils, as well as the status of T cell infiltration. In the animal studies of $T_{\rm reg}$ cell depletion presented here, T cell–mediated tumor rejection depended on co-infiltrating eosinophils. It will be of interest to determine whether eosinophils are also involved in other approaches of T cell–based tumor rejection. In this context, we note that in patients with melanoma, blockade of the immunological 'checkpoint' consisting of the immunomodulatory receptor CTLA-4 (CD152) with ipilimumab, an antibody to CTLA-4, induces an early increase in lymphocyte and eosinophil counts associated with improved survival⁴³. However, the precise role of eosinophils in this setting remains to be evaluated.

In the past few years much progress has been made in the development of improved vaccine formulations, adoptive T cell transfer and inhibitors of immunological checkpoints, but the clinical success of tumor immunotherapy is still limited. Increasing evidence indicates that limited access of effector T cells into tumors is a major hurdle for successful immunotherapy 44,45. On the basis of our study, and owing to their tumor-homing properties, eosinophils might now emerge as a promising tool for the improvement of clinical cancer immunotherapy.

METHODS

Methods and any associated references are available in the online version of the paper.

Note: Any Supplementary Information and Source Data files are available in the online version of the paper.

ACKNOWLEDGMENTS

We thank S. Schmitt for technical assistance; L. Umansky for multiplex analysis of cytokines; and T. Tüting (University of Bonn) for HCmel melanoma cells. Supported by Wilhelm Sander Stiftung (2009.022.2 to G.J.H.), the Cooperation Program in Cancer Research by the German Cancer Research Center, the Israel Ministry of Science, Technology and Space (G.J.H.) and the Bonn Cluster of Excellence to (N.G.).

AUTHOR CONTRIBUTIONS

R.C., I.M.S., N.G., P.B. and G.J.H. designed the experimental plan; R.C., I.M.S. and O.C.S. performed the experiments; and R.C., I.M.S. and G.J.H. wrote the manuscript.

COMPETING FINANCIAL INTERESTS

The authors declare no competing financial interests.



Reprints and permissions information is available online at http://www.nature.com/ reprints/index.html.

- Rothenberg, M.E. & Hogan, S.P. The eosinophil. Annu. Rev. Immunol. 24, 147-174
- Rosenberg, H.F., Dyer, K.D. & Foster, P.S. Eosinophils: changing perspectives in health and disease. Nat. Rev. Immunol. 13, 9-22 (2013).
- Kita, H. Eosinophils: multifaceted biological properties and roles in health and disease. Immunol. Rev. 242, 161-177 (2011).
- 4. Melo, R.C., Liu, L., Xenakis, J.J. & Spencer, L.A. Eosinophil-derived cytokines in health and disease: unraveling novel mechanisms of selective secretion. Allergy 68, 274-284 (2013).
- Reinbach, G. Ueber das Verhalten der Leukocyten bei malignen Tumoren. Arch. Klin. Chir 46, 486-562 (1893).
- Simson, L. et al. Regulation of carcinogenesis by IL-5 and CCL11: a potential role for eosinophils in tumor immune surveillance. J. Immunol. 178, 4222-4229
- Cormier, S.A. et al. Pivotal advance: eosinophil infiltration of solid tumors is an early and persistent inflammatory host response. J. Leukoc. Biol. 79, 1131-1139
- Lotfi, R. et al. Eosinophils oxidize damage-associated molecular pattern molecules derived from stressed cells. J. Immunol. 183, 5023-5031 (2009).
- Lotfi, R., Lee, J.J. & Lotze, M.T. Eosinophilic granulocytes and damage-associated molecular pattern molecules (DAMPs): role in the inflammatory response within tumors. J. Immunother. 30, 16-28 (2007).
- 10. Davis, B.P. & Rothenberg, M.E. Eosinophils and cancer. Cancer Immunol. Res. 2, 1-8 (2014).
- 11. Gatault, S., Legrand, F., Delbeke, M., Loiseau, S. & Capron, M. Involvement of eosinophils in the anti-tumor response. Cancer Immunol. Immunother. 61, 1527-1534 (2012).
- 12. Tepper, R.I., Coffman, R.L. & Leder, P. An eosinophil-dependent mechanism for the antitumor effect of interleukin-4. Science 257, 548-551 (1992).
- 13. Golumbek, P.T. et al. Treatment of established renal cancer by tumor cells engineered to secrete interleukin-4. Science 254, 713-716 (1991).
- 14. Noffz, G., Qin, Z., Kopf, M. & Blankenstein, T. Neutrophils but not eosinophils are involved in growth suppression of IL-4-secreting tumors. J. Immunol. 160, 345–350
- 15. Mattes, J. et al. Immunotherapy of cytotoxic T cell-resistant tumors by T helper 2 cells: an eotaxin and STAT6-dependent process. J. Exp. Med. 197, 387-393 (2003).
- 16. Samoszuk, M. et al. Increased blood clotting, microvascular density, and inflammation in eotaxin-secreting tumors implanted into mice. Am. J. Pathol. 165, 449-456 (2004).
- 17. Krüger-Krasagakes, S., Li, W., Richter, G., Diamantstein, T. & Blankenstein, T. Eosinophils infiltrating interleukin-5 gene-transfected tumors do not suppress tumor growth. Eur. J. Immunol. 23, 992-995 (1993).
- 18. Huland, E. & Huland, H. Tumor-associated eosinophilia in interleukin-2-treated patients: evidence of toxic eosinophil degranulation on bladder cancer cells. J. Cancer Res. Clin. Oncol. 118, 463–467 (1992).
- 19. Sosman, J.A. et al. Evidence for eosinophil activation in cancer patients receiving recombinant interleukin-4: effects of interleukin-4 alone and following interleukin-2 administration. Clin. Cancer Res. 1, 805-812 (1995).
- 20. Galdiero, M.R. et al. Tumor associated macrophages and neutrophils in cancer. Immunobiology 218, 1402-1410 (2013).
- 21. Li, X., Kostareli, E., Suffner, J., Garbi, N. & Hammerling, G.J. Efficient Treg depletion induces T-cell infiltration and rejection of large tumors. Eur. J. Immunol. 40 3325-3335 (2010)

- 22. Zimmermann, N. et al. Siglec-F antibody administration to mice selectively reduces blood and tissue eosinophils. Allergy 63, 1156-1163 (2008).
- 23. Chu, V.T. et al. Eosinophils are required for the maintenance of plasma cells in the bone marrow. Nat. Immunol. 12, 151-159 (2011).
- 24. Hamzah, J. et al. Vascular normalization in Rgs5-deficient tumours promotes immune destruction. Nature 453, 410-414 (2008).
- 25. Munitz, A. & Levi-Schaffer, F. Eosinophils: 'new' roles for 'old' cells. Allergy 59, 268-275 (2004).
- 26. Restifo, N.P., Dudley, M.E. & Rosenberg, S.A. Adoptive immunotherapy for cancer: harnessing the T cell response. Nat. Rev. Immunol. 12, 269-281 (2012)
- 27. Jain, R.K. Normalization of tumor vasculature: an emerging concept in antiangiogenic therapy. Science 307, 58-62 (2005).
- 28. Dalton, D.K. et al. Multiple defects of immune cell function in mice with disrupted interferon-gamma genes. Science 259, 1739-1742 (1993).
- 29. Stockmann, C. et al. Deletion of vascular endothelial growth factor in myeloid cells accelerates tumorigenesis. Nature 456, 814-818 (2008).
- 30. Stockmann, C., Schadendorf, D., Klose, R. & Helfrich, I. The impact of the immune system on tumor: angiogenesis and vascular remodeling. Front. Oncol. 4, 69 (2014).
- 31. Huang, Y., Goel, S., Duda, D.G., Fukumura, D. & Jain, R.K. Vascular normalization as an emerging strategy to enhance cancer immunotherapy. Cancer Res. 73, 2943-2948 (2013).
- 32. Ganss, R., Ryschich, E., Klar, E., Arnold, B. & Hammerling, G.J. Combination of T-cell therapy and trigger of inflammation induces remodeling of the vasculature and tumor eradication. Cancer Res. 62, 1462-1470 (2002).
- 33. Ryschich, E., Schmidt, J., Hammerling, G.J., Klar, E. & Ganss, R. Transformation of the microvascular system during multistage tumorigenesis. Int. J. Cancer 97, 719-725 (2002).
- 34. Facciabene, A. et al. Tumour hypoxia promotes tolerance and angiogenesis via
- CCL28 and T_{reg} cells. *Nature* **475**, 226–230 (2011). 35. Gabrilovich, D.1., Ostrand-Rosenberg, S. & Bronte, V. Coordinated regulation of myeloid cells by tumours. Nat. Rev. Immunol. 12, 253-268 (2012).
- 36, Klug, F. et al. Low-dose irradiation programs macrophage differentiation to an iNOS+/M1 phenotype that orchestrates effective T cell immunotherapy. Cancer Cell 24. 589-602 (2013).
- 37. Garbi, N., Arnold, B., Gordon, S., Hammerling, G.J. & Ganss, R. CpG motifs as proinflammatory factors render autochthonous tumors permissive for infiltration and destruction. J. Immunol. 172, 5861-5869 (2004).
- 38. Finlay, D.K. et al. PDK1 regulation of mTOR and hypoxia-inducible factor 1 integrate metabolism and migration of CD8+ T cells. J. Exp. Med. 209, 2441-2453 (2012).
- 39. Shi, S. et al. Combining antiangiogenic therapy with adoptive cell immunotherapy exerts better antitumor effects in non-small cell lung cancer models. PLoS ONE 8, e65757 (2013).
- 40. Huang, Y. et al. Vascular normalizing doses of antiangiogenic treatment reprogram the immunosuppressive tumor microenvironment and enhance immunotherapy. Proc. Natl. Acad. Sci. USA 109, 17561-17566 (2012).
- 41. Liu, L.Y. et al. Generation of Th1 and Th2 chemokines by human eosinophils: evidence for a critical role of TNF-α. J. Immunol. 179, 4840-4848 (2007).
- 42. Wu, D. et al. Eosinophils sustain adipose alternatively activated macrophages associated with glucose homeostasis. Science 332, 243-247 (2011).
- 43. Delyon, J. et al. Experience in daily practice with ipilimumab for the treatment of patients with metastatic melanoma: an early increase in lymphocyte and eosinophil counts is associated with improved survival. Ann. Oncol. 24, 1697-1703 (2013).
- 44. Motz, G.T. & Coukos, G. Deciphering and reversing tumor immune suppression. Immunity 39, 61-73 (2013).
- 45. Fridman, W.H. et al. Prognostic and predictive impact of intra- and peritumoral immune infiltrates. Cancer Res. 71, 5601-5605 (2011).



ONLINE METHODS

Mice. C57BL/6N mice, transgenic Foxp3.LuciDTR-4 BAC mice (DTR4)⁴⁶, OT-I mice (with transgenic expression of T cell receptor specific for the epitope of ovalbumin amino acids 257–264 and restricted to MHC class I)⁴⁵ and $Rag2^{-/-}$ mice (deficient in recombination-activating gene 2) were bred at the central animal facility of the German Cancer Research Center and held under specific pathogen–free conditions. 6- to 8-week-old mice were used for experiments. Experiments were conducted according to governmental and institutional guidelines and regulations (Regierungspräsidium Karlsruhe, permit no. 35-9185.81/G98/08 and 35-9185.81/G206/12). The number of mice per group was confirmed by the statistical department of the Deutsches Krebsforschungszentrum.

Tumor challenge and cell depletion in mice. The OVA-expressing B16 melanoma MO4, MC38 adenocarcinoma, RMA thymoma, 3LL Lewis lung carcinoma and HCmel1274 melanoma were used. The HCmel1274 melanoma line is derived from genetically modified Hgf-Cdk4 mice that develop cutaneous melanoma 47 . Tumor lines were mycoplasma free. Mouse abdomens were given intradermal inoculation of 1×10^6 tumor cells. Tumor sizes were measured with a caliper every 3 d, and tumor volume was calculated according to the following formula: volume = 0.5 \times length \times width². Mice were killed when the tumor volume reached 2,000 mm³. Measurements were performed by a researcher unaware of the allocation of mice into groups.

For the depletion of T_{reg} cells, transgenic Foxp3.LuciDTR-4 BAC mice received intraperitoneal injection of diphtheria toxin (Sigma-Aldrich) at a dose of 15 ng per gram body weight. The depletion of T_{reg} cells was initiated 8 d after injection of tumors, when tumors exhibited a volume of 100–300 mm³. For the depletion of eosinophils, 15 μg anti Siglec-F (238047; R&D Systems) was injected intraperitoneally 2, 4, 5 and 6 d after depletion of T_{reg} cells.

Tumor Isolation. Tumor samples for analysis were isolated from mice at the onset of tumor rejection, before any sign of rejection was observed, and mice from the different groups showed similar tumor volumes. Tumors were analyzed at day 13, 6 d after the depletion T_{reg} cells or 2 d after the co-transfer of CD8+ T cells.

Tissue digestion for population analyses and cell sorting. Tissues were isolated from the mice and placed in 3 ml of PBS containing 100 U/ml of collagenase IV and 1 mg/ml of DNase I. Tissues were disrupted through the use of forceps and were incubated at 20 °C with gentle stirring with a magnet (100 r.p.m.). After 30 min, samples were filtered through a 40- μm filter. Erythrocytes were removed by incubation for 1 min with ACK buffer (Dulbecco's PBS containing 0.15 M NH₄Cl, 10 mM KHCO₃ and 0.1 mM EDTA). Cells were next incubated for 15 min in blocking buffer (flow cytometry buffer (Dulbecco's PBS containing 2.5% FCS) buffer with 1% normal immunoglobulin (Privigen; CSL Behring). Samples were then stained for analysis by flow cytometry and cell sorting.

In vitro activation of CD8+ T cells and adoptive transfer. Spleens and peripheral lymph nodes were collected from naive OT-I mice and were dissociated to obtain single-cell suspensions. Red blood cells were lysed with ACK buffer. Cells were resuspended at a density of 1×10^6 cells per ml in RPMI-1640 medium supplemented with 10% FCS, 2 nM glutamine, 100 U/ml penicillin, 100 µg/ml streptomycin, 0.05 mM 2-mercaptoethanol, 10 U of recombinant IL-2 per ml and 25 nM SIINFEKL. Cells were used for adoptive transfer 3 d after activation. Mice received intravenous injection of 2.5×10^6 activated CD8+ T lymphocytes 1 d after eosinophil transfer and 4 and 8 d after the first transfer.

Eosinophil purification, *in vitro* activation, labeling and adoptive therapy. Brewer's thioglycollate broth (4%; Becton Dickinson) was autoclaved and then was 'aged' at 20 °C for at least 1 month before use. Mice were killed 3 d after intraperitoneal injection of 1 ml 4% thioglycollate. Peritoneal cells were collected by peritoneal lavage with PBS. Freshly isolated cells from the peritoneal cavity were stained with phycoerythrin-conjugated anti-Siglec-F (E50-2440; BD Biosciences), washed with MACS running buffer (Miltenyi Biotec) and incubated with anti-phycoerythrin microbeads according to the

manufacturer's instructions (Miltenyi Biotec). Eosinophils were purified on a quadroMACS (Miltenyi Biotec). Purified eosinophils were counted, then were washed and resuspended at 1×10^6 cells per ml in RPMI-1640 medium supplemented with 10% FCS, 2 nM glutamine, 100 U/ml penicillin/100 μg/ml streptomycin and 0.05 mM 2-mercaptoethanol and then activated with 15 ng/ml of mIFN- γ and 15 ng/ml of mTNF. 16 h later, cells were collected and the purity and viability of Siglec-F+ cells were analyzed by flow cytometry. Purity was usually >90%. For adoptive transfer, 5×10^6 cells in 200 μ l of PBS were injected intravenously when the tumor volume had reached 200-400 mm³. Fresh preparations of activated eosinophils were injected again 4 d and 8 d after the first transfer. For the transfer of non-activated eosinophils, eosinophils were cultured for 4 h in complete RPMI medium (RPMI medium containing FCS (10%), L-glutamine (2 mM), sodium pyruvate (2 mM), penicilin and streptavidin (100 µg/ml), 2-mercaptoetanol (0.1 mM) and HEPES (10 mM)) without mouse IFN- γ or mouse TNF. For tracking of transferred eosinophils, either CD45.1 $^+$ mice were used or cells were incubated for 15 min at 4 $^\circ$ C in 2 μ M CFSE (carboxyfluorescein diacetate succinimidyl ester), washed and resuspended in PBS. 5×10^6 eosinophils were injected intravenously and labeled eosinophils in isolated tissues were quantified by flow cytometry.

In vitro migration assay. Migration was assessed in 24-well Transwell plates with a 5-μm pore size (Corning Life Sciences). The lower chamber was loaded with 600 μ l migration medium (RPMI-1640 medium supplemented with 0.2% FCS, 2 nM glutamine, 100 U/ml penicillin/100 μ g/ml streptomycin and 0.05 mM 2-mercaptoethanol) containing 1×10^6 activated eosinophils or with supernatants derived from eosinophils cultured overnight. 1×10^5 effector cells (naive or activated OT-I CD8+ cells) were added in a volume of 100 μl of migration medium to the upper chamber. For dose-response curves, eosinophils were 'titrated' in the lower chamber from a density of 0.25×10^6 in $600\,\mu l$ to 8×10^6 in 600 µl. As a positive control, effector cells were placed directly into the lower chamber. As a negative control, migration medium alone was placed in the upper chamber. As a control group, OT-I CD8+ cells (at a density of 1×10^5 cells per 100 μ l) were added to the upper chamber and migration medium alone was added to the lower chamber. Plates were incubated for 5 h at 37 °C in 5% CO₂. Thereafter, the Transwell inserts were removed and the contents of the lower compartment were carefully recovered. Cells from the lower chamber were stained for specific markers (antibodies identified below) and the cells were quantified by flow cytometry in the presence of a known number of microbeads. The migration rate was calculated as follows: 100 × (number of cells from lower chamber/number of beads) / (number of cells from input sample/number of beads). For experiments in which the activity of specific chemokines was blocked, the migration index was calculated as follows: migration in the presence of activated eosinophils plus antibody to chemokine / migration in the presence of activated eosinophils without antibody.

Chemokine blockade. For the evaluation of chemokine-specific migration, neutralizing antibodies to chemokines (anti-CCL5 (53405), anti-CXCL9 (49106) and anti-CXCL10 (134013); all 20 μ g/ml, and all from R&D Systems) or the appropriate isotype-matched control antibody (mouse IgG2a (2A3) and goat IgG (603-298-8564), both from BioXCell) were added to the lower chamber before the chemotactic assay. For *in vivo* blockade, anti-CCL5, anti-CXCL9, anti-CXCL10 or the appropriate isotype-matched controls was injected (250 μ g per mouse) every second day.

Flow cytometry and cell sorting. The following fluorochrome-conjugated antibodies were used: anti-CD3 (145-2C11), anti-CD4 (GK1.5), anti-CD8 (53-6.7) and anti-NK1.1 (PK136) (all from BD Biosciences); anti-Siglec-F (E50-2440), anti-Ly6C (AL-21), anti-Ly6G (1A8), anti-CD19 (1D3) and anti-CD90.1 (HI551) (all from eBioscience); and anti-CD4 (RM4-5), anti-I-A/I-E (M5/114.15.2), anti-Gr-1 (RB-6-8C5), anti-CD44 (IM7), anti-CD62L (MEL-14), anti-CD45.1(A20), anti-CD45.2 (104) and anti-CD69 (H1.2F3) (all from Biolegend). Propidium iodide (Sigma-Aldrich) was used as viability dye. Labeled cells were analyzed on a FACSCanto II flow cytometer (BD Biosciences) and were evaluated with FlowJo Mac software, version .8.2 (TreeStar). For analysis of cells purified from tumors, 3×10^4 to 5×10^4 cells were sorted with a FACSAria II (BD Biosciences).



NATURE IMMUNOLOGY doi:10.1038/ni.3159

Quantitative RT-PCR. RNA from tumors and eosinophils (isolated by magnetic-activated cell sorting) was isolated with an RNeasy Mini kit (Qiagen), followed by cDNA synthesis with SuperScript II reverse transcriptase (Invitrogen). RNA from macrophages and eosinophils sorted by flow cytometry (purity >95%) was isolated with an RNeasy Micro kit (Qiagen), followed by cDNA synthesis with an iScript cDNA synthesis kit (Bio-Rad). Gene expression was assessed by real-time PCR with Thermo SYBR green/ROX (Thermo Scientific) and primers (Supplementary Table 1) in a 7500 Real time PCR system (Applied Biosystems). Polymerase was activated at 95 °C for 10 min. Samples were amplified by 40 cycles of 10 s at 95 °C and 1 min at 60 °C. Dissociation curves were used to confirm specificity of the PCR. Results were calculated by the change-in-cycling-threshold ($\Delta\Delta Ct$) method as follows (relative to the control gene Gapdh, encoding glyceraldehyde phosphate dehydrogenase): $-\Delta\Delta Ct = 2 - \Delta Ct$ sample $-\Delta Ct$ biggest Ct, where $\Delta Ct = Ct$ target mRNA - Ct Gapdh mRNA. PCR was performed by an independent researcher unaware of sample group allocation.

Protein analysis. Tumor tissue and purified eosinophils were lysed with a Bio-Plex Cell Lysis Kit (Bio-Rad) and were processed as described⁴⁸. Cytokines were quantified with multiplex protein array system technology according to the manufacturer's protocol (Bio-Rad).

Tumor cryopreservation. Tumors were carefully removed from mice that had been killed and were placed in optimum cutting temperature gel (Tissue-Tek; Sakura). For homogeneous cryopreservation, samples were incubated for 10 min at 4 °C and then were placed in liquid nitrogen–cooled isopentane for 10 min. Thereafter, samples were slowly introduced into liquid nitrogen. Sections from the tumors 5 μm in thickness were cut on a Leica CM3050S cryotome, then were dried overnight and fixed by 10 min of incubation in cold acetone.

Vasculature and immunohistofluorescence analysis. For immunofluorescence staining, samples were preincubated for 15 min in blocking buffer. Blocking buffer was removed and the samples were incubated for 60 min at 20 °C with primary antibodies (hamster anti–mouse CD31 (2H8; BioRad); rat anti–mouse CD31 (390), rat anti–mouse CD8 (56-3.7), rat anti–mouse CD106 (429) and phycoerytherin–anti-CD8 (5H10; all from Biolegend); mouse antibody to α -smooth muscle antigen(1A4; eBiosciences); and Brilliant Violet 421–anti-Siglec-F (E50-2440; BD Biosciences). Excess antibody was removed by washing for 5 min in PBS containing 0.01% Tween 20 (PBS-Tween). Secondary antibody (indocarbocyanine-labeled goat anti-rat IgG (Poly4054)or fluorescein isothiocyanate–labeled goat anti-hamster IgG (Poly4055); both from Biolegend) was added, and samples were incubated in the dark for 60 min at 20 °C. Excess antibody was removed by washing for

5 min in PBS-Tween. The staining of α -smooth muscle actin was amplified by use of a 'mouse-on-mouse' M.O.M. kit (Vector). Samples were mounted with Vectashield mounting medium for fluorescence with DAPI (4,6-diamidino-2-phenylindole; Vector).

For hypoxia studies a Hypoxyprobe kit was used. 2 mg pimonidazole was injected intravenously and was left to circulate for 20 min. Staining of tumor cryosections was performed with a Hypoxyprobe Plus Kit according to the supplier' protocol. For perfusion experiments, mice were given retro-orbital injection of 50 μg of fluorescein isothiocyanate–labeled tomato lectin (*Lycopersicon esculentum*; Vector). After 10 min of circulation, the mouse heart was perfused with PBS, followed by 2% (wt/vol) PFA, and tumors were frozen in optimum cutting temperature compound (Leica). For evaluation of vessel leakiness, 1 mg of 70-kDa fluorescein isothiocyanate–dextran (Invitrogen) was injected retro-orbitally into mice and was allowed to circulate for 10 min. The mouse heart was perfused with PBS, followed by 2% (wt/vol) PFA, and tumors were frozen in optimum cutting temperature compound. Mice were anesthetized with 200 μ l of 0.5% Rompun (wt/vol) and 25 mg/ml Ketavet before injection of the reagents.

A Zeiss Axio Observer.Z1 microscope (Zeiss) was used for the visualization of stained sections. ZEN Blue software (Zeiss)was used for analysis. Vessel were counted in ten independent 1,250- μm^2 sections from each mouse. Vessel size was quantified by analysis of 100–300 vessels from independent mice. The localization of VCAM-1 (CD106), tomato lectin or α -smooth muscle actin together with CD31 was measured with the colocalization tool from the ZEN Blue software, whereby colocalization = CD31+ target-positive pixels / CD31+ pixels. For analysis of leakiness, the percentage of the field covered by dextran was measured with Zeiss blue software.

Statistical analysis. The Kolmogorov–Smirnov test was performed to ensure normal distribution. The Levene test was performed to ensure homogeneity of variance. Comparisons between two groups were assessed by Student's *t*-test. Comparisons of tumor-growth curves were assessed by analysis of variance. Survival studies were assessed by Kaplan-Meier curves and the log-rank (Mantel-Cox) test. Data were analyzed with Prism 5 software (GraphPad). *P* values lower than 0.05 were considered statistically significant.

- Suffner, J. et al. Dendritic cells support homeostatic expansion of Foxp3+ regulatory T cells in Foxp3.LuciDTR mice. J. Immunol. 184, 1810–1820 (2010).
- Kohlmeyer, J. et al. Complete regression of advanced primary and metastatic mouse melanomas following combination chemoimmunotherapy. Cancer Res. 69, 6265–6274 (2009).
- Domschke, C. et al. Intratumoral cytokines and tumor cell biology determine spontaneous breast cancer-specific immune responses and their correlation to prognosis. Cancer Res. 69, 8420–8428 (2009).



doi:10.1038/ni.3159

Corrigendum: Eosinophils orchestrate cancer rejection by normalizing tumor vessels and enhancing infiltration of CD8+ T cells

Rafael Carretero, Ibrahim M Sektioglu, Natalio Garbi, Oscar C Salgado, Philipp Beckhove & Günter J Hämmerling *Nat. Immunol.* 16, 609–617 (2015); published online 27 April 2015; corrected online 21 May 2015

In the version of this article initially published, the description of the data presented in Figure 4f–i was incorrect. That section of Results should read as follows: "The additional depletion of eosinophils…resulted in increased tumor hypoxia….(Fig. 4f and Supplementary Fig. 6). Depletion of eosinophils also increased vascular leakiness and diminished vascular perfusion…(Fig. 4g–i and Supplementary Fig. 6)." The errors have been corrected in the HTML and PDF versions of the article.



Corrigendum: Eosinophils orchestrate cancer rejection by normalizing tumor vessels and enhancing infiltration of CD8+ T cells

Rafael Carretero, Ibrahim M Sektioglu, Natalio Garbi, Oscar C Salgado, Philipp Beckhove & Günter J Hämmerling *Nat. Immunol.* 16, 609–617 (2015); published online 27 April 2015; corrected online 21 May and 13 November 2015

In the version of this article initially published, the graph in Figure 2e was incorrect. This has been replaced with the correct graph. The error has been corrected in the HTML and PDF versions of the article.